Polymer Chemistry

Accepted Manuscript

ROYAL SOCIETY OF CHEMISTRY

www.rsc.org/polymers

Cite this: DOI: 10.1039/c0xx00000x

www.rsc.org/xxxxxx

ARTICLE TYPE

Synthesis of triphenylamine based polysiloxane as blue phosphorescent host

Dianming Sun,[a] Zhaomin Yang,[a] Xiaoli Sun,[a] Huihui Li,[a] Zhongjie Ren,[a] * Junteng Liu, [b] * Dongge Ma,[c] and Shouke Yan [a] *

Received (in XXX, XXX) Xth XXXXXXXXX 200X, Accepted Xth XXXXXXXXX 200X
DOI: 10.1039/b000000x

In this work, a triphenylamine based polysiloxane (PTPAMSi) has been successfully synthesized. The PTPAMSi exhibits a high decomposition temperature (T_d= 377 °C) and glass transition temperature (T_g = 63 °C). It also dispalys good film-forming ability, high morphological stability and good miscibility with the dopant FIrpic as revealed by atomic force microscopy (AFM). The silicon-oxygen linkage of PTPAMSi disrupts its conjugation and results in a sufficiently high triplet energy level (E_T = 2.9 eV). A FIrpic-based device using PTPAMSi as a host shows a turn-on voltage of 6.8 V, maximum external quantum efficiency of 3.8%, maximum current efficiency of 7.6 cd/A. These results demonstrate that using polysiloxane to modify triphenylamine is a promising approach to improve the physcial properties of triphenylamine while maintain its photophyscial and electrochemical properties.

Introduction

Triarylamines are a class of high-performance organic hole transporting materials and play an important role in novel organic electronic devices.[1-3] Many methods have been used to improve their physical properties with maintaining the charge carrier mobility of these materials.[4, 5] Bender's group has recently shown that siliconized triarylamines can be considered as traditional organic semiconductors as they follow the conventional theory concerning charge carrier transport.[6-8] These siliconized triarylamines liquid organic semiconductors with the mechanical flexibility and improved interfacial properties may enable new innovations in solid-state organic lighting,[9] organic light emitting diodes[10] and organic photovoltaics.[11] Mark used triarylamine siloxane to modify anode as hole injection layers and obtained high efficiency/high luminance small molecule green- and blue-organic light-emitting diodes.[12] Moreover, photorefractive properties of poly(siloxane)-triarylamine-based composites for high-speed applications have been researched.[13] Theato et. al employed the poly(methylsilsesquioxane)-poly(N,N-di-4-methylphenylamino styrene) as a potential hole-injection layer forming material, which resulted in an effective planarization of the anode interface for optoelectronic applications through spin-coating and thermally induced crosslinking.[14] However, the siloxane modified triarylamines for electrophosphorescent hosts have not been reported yet.

Organic light emitting diodes (OLEDs) that harvest both singlet and triplet excitons, leading to an internal quantum efficiency of 100%, have been realized by using phosphorescent dyes such as iridium bis(4,6-difluorophenyl)pyridinato-N,C^2 picolinate (FIrpic).[15,16] In general, high efficiency phosphorescent organic light emitting diodes (PhOLEDs) are based on the host-guest strategy where a triplet emitter is dispersed homogeneously in a suitable host matrix to prevent self-quenching and triplet-triplet annihilation.[17] To date, internal quantum efficiencies of 100% have been realized for green and red phosphorescent OLEDs,[18,19] but extensive research continues for ideal host materials for blue PhOLEDs. An ideal host for blue PhOLEDs should possess sufficiently high triplet energy (E_T >2.7 eV) to confine triplet excitons within the emitting layer and avoid reverse energy transfer from guest to host.[20] The host should also possess high thermal, electrochemical, and morphological stability and good film-forming ability to realize devices with high performance.[21] Tremendous efforts have been devoted to the phosphorescent polymeric light emitting diodes (PhPLEDs) because of their capability of harvesting both singlet and triplet excitons which can lead to an internal quantum efficiencies of 100% by using phosphorescent dyes.

It has been reported that applying polysiloxane to modify triarylamines would not affect the photophysical and electrochemical characteristics of the triarylamine.[22] The polysiloxane is a fascinating polymer with good solubility in common organic solvents, good film-forming ability, fair adhesion to various substrates and excellent resistances to thermal, chemical and irradiation degradation. To improve thermal, electrochemical, and morphological stability and good film-forming ability of organic semiconductors, incorporation of siloxanes into organic semiconductor molecular structures has been successful. Meanwhile this method would not affect the electronic properties of organic semiconductors. Enlighten by this, we try synthesizing triarylamines based polysiloxanes for host materials of blue PhOLEDs. However, the previous siloxanes modified triarylamines are small molecule liquid,[7,8] corsslinked structure[23] or triarylamines with low content by post-functionality of silicon polymers,[22] which cannot meet the requirement of electrophosphorescent host materials.

Herein, we have first successfully attached the N, N-diphenylaniline moieties into siloxane and then obtained polymer PTPAMSi by polycondensation. PTPAMSi possesses a sufficiently high E_T of 2.9 eV. A blue phosphorescent device containing this novel host was formed by solution processing. This device displayed a maximum current efficiency of 7.6 cd/A (1.9 lm/W, 3.8%). In addition, the new host possesses a high

degradation temperature, excellent film-forming ability and good compatibility with FIrpic.

Results and Discussion

Synthesis and Characterization

The synthetic route and chemical structures of 4-(diethoxy(methyl)silyl)-N,N-diphenylaniline(2) and PTPAMSi(4) are depicted in Scheme 1. The starting material 4-bromo-N,N-diphenylaniline (1) was obtained from commercial source. Transformation of (1) to (2) was achieved by Barbier-Grignard reaction with methyldiethyoxylchlorosilane. (4-(diphenylamino)phenyl)(methyl)silanediol (3) could be obtained by subsequent acid hydrolysis in dilute THF-HCl solution at 0 °C.

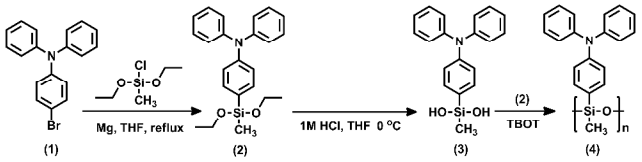

Scheme 1 Synthetic route for PTPAMSi

The desired polymer PTPAMSi was easily synthesized by dealcoholization condensation from the corresponding diethoxy monomer (OEt-Si) (2) and dihydroxy monomer (OH-Si) (3) under tetrabutyltitanate (TBOT) catalyzed polycondensation as shown in the experimental section. The end groups were blocked with trimethylchlorosilane to stabilize the resultant polysiloxane. After the end of polymerization, the solution was concentrated and precipitated in methanol to give the product as white powders. ^{1}H, ^{13}C and ^{29}Si NMR spectroscopies and element analysis were employed to confirm the chemical structures of the compounds as described in the experimental section. The resulting polymer (4) was fully characterized by ^{1}HNMR spectroscopy and gel permeation chromatography (GPC). The weight average molecular weight was determined to be 9.34 kDa with a narrow polydispersity index of 1.51 by GPC in THF using polystyrene as a standard. The obtained product is highly soluble in common organic solvents such as chloroform, tetrahydrofuran, toluene and chlorobenzene. Therefore, it can be easily fabricated into film by solution casting, spin-coating, and dipping techniques.

Thermal properties

The thermal properties of PTPAMSi measured by thermogravimetric analysis (TGA) and differential scanning calorimetry (DSC) are shown in Figure 1 and summarized in Table 1. TGA measurement reveals a high thermal decomposition temperature of 377 **°C** with the 5% weight-loss temperature (Figure 1a). The high thermal stability is probably due to the polysiloxane backbone. From DSC trace, only a glass transition area occurs in the range of 30-180 **°C** without melting or crystallization peaks, which suggests an amorphous state with a distinct glass transition temperature (T_g) of 63 **°C** during the second heating scan (Figure 1b). The amorphous property and low glass transition temperature should be caused by the flexible polysiloxane backbone. Because the Si-O bond length is about 1.64 Å, which is significantly longer than C-C bond length of 1.54 Å, and the Si-O-Si bond angle of 143° is also significantly larger than the usual C-C bond angle of 109.5°. Otherwise, no substituent groups on oxygen atom results in better flexibility.[24]

The amorphous nature of PTPAMSi is resistant to crystallization and phase disengagement, which is desirable for OLEDs with high stability and efficiency.

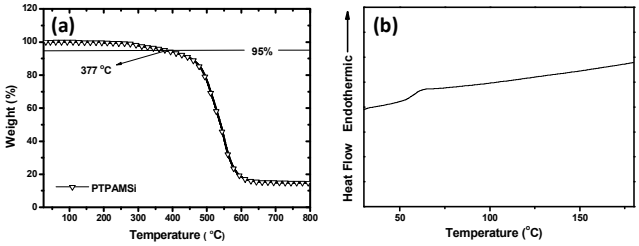

Fig. 1 (a) TGA thermogram of PTPAMSi recorded at a heating rate of 10 °C min^{-1} under nitrogen atmosphere. (b) DSC trace of PTPAMSi recorded at a heating rate of 10 °C min^{-1} under nitrogen atmosphere.

Morphological properties

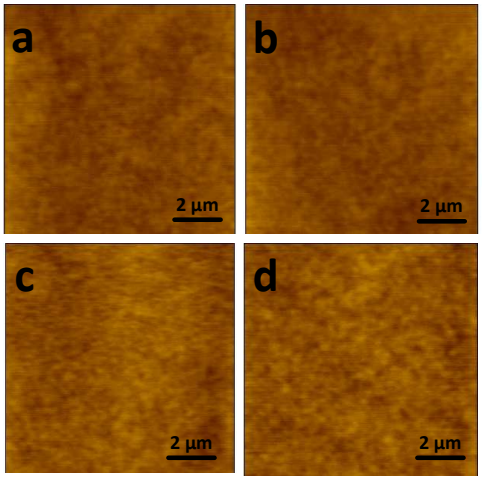

Fig. 2 AFM topographic images of a solution processed film doped with 10% FIrpic for PTPAMSi (a) unannealed (b) annealed at 90 °C for 12h (c) annealed at 90 °C for 24h and (d) annealed at 90 °C for 48h.

The film-forming ability, morphological stability of PTPAMSi and miscibility to the dopant FIrpic were also investigated by the atomic force microscopy (AFM). As shown in Figure 2a, the AFM image of 10 wt% FIrpic doped PTPAMSi film displays smooth and homogeneous morphology with small value of root-mean-square (RMS) roughness of 0.23 nm. It is free of particle aggregation or phase separation, suggesting the good film-forming ability and good miscibility to the FIrpic. To further investigate the thermal stability, the film was then annealed at 90 °C for 12 hours as shown in Figure 2b, which is higher than the corresponding T_g. surface roughness was changed a little from 0.23 nm to 0.27 nm, however, as time went on at the same temperature, almost no change can be observed (Figure 2c, 2d). The excellent stability of film morphology appears to be a result of its polysiloxane backbone, which should be capable of keeping film integrity throughout the entire fabrication and operation process.

Photophysical properties

Figure 3a shows the ultraviolet-visible (UV-vis) absorption and photoluminescence (PL) emission spectra of PTPAMSi in dilute

CH_2Cl_2 solution and thin films, as well as the phosphorescence (Phos) spectra measured in a frozen dichloromethane matrix at 77 K. In CH_2Cl_2, the strong absorption band around 305 nm can be assigned to the triphenylamine pendant n-π* transition[25] and almost no solvatochromism is observed. Besides, no significant charge transfer absorption band between each arylamine segment indicates the disruption of the π-conjugation because of the polysiloxane main chain. In addition, from the threshold of the solid-state absorption spectrum, the energy gap (E_g) of PTPAMSi can be calculated to be 3.55 eV.

In CH_2Cl_2 solution, PTPAMSi exhibits clear near-ultroviolet vibronic feature with an emission peak at around 365 nm. As compared to solution emission spectrum, the emission of PTPAMSi thin film display pronounced dual emission bands, the emission peak at around 365 nm, which is the same as in dichloromethane, can be assigned to the π-π* transition; the unclear emission at longer wavelength may be due to aggregate and excimer emission.[26]

The phosphorescence spectrum was measured in a frozen dichloromethane matrix at 77K, and the triplet energy (E_T) of PTPAMSi was estimated as 2.9 eV from the highest energy vibronic band of the phosphorescence spectrum, and the triplet enegy level is significantly higher than that of blue phosphor FIrpic ensuring that PTPAMSi can be used as a suitable host material.

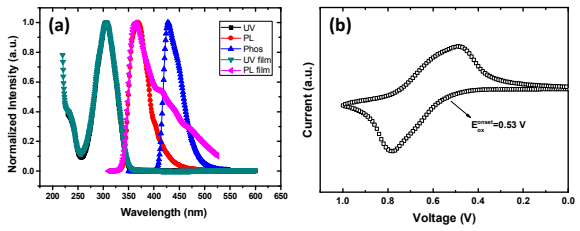

Fig. 3 (a) The absorption and emission spectra of PTPAMSi in dichloromethane at 5×10^{-6} M and PTPAMSi thin film at room temperature, phosphorescence spectrum of PTPAMSi in dichloromethane at 77 K. (b) Cyclic voltammogram of PTPAMSi in CH_3CN for oxidation scan.

Electrochemical properties

The electrochemical behavior of PTPAMSi was investigated by cyclic voltammetry using tetra (n-butyl) ammonium hexafluorophosphate (0.1 M) as a supporting electrolyte in anhydrous CH_2Cl_2 as shown in Figure 3b and the results are summarized in Table 1. During the anodic scan, one reversible oxidation couple at relatively low positive potentials with E_{ox}^{onset} of 0.53 V, which originates from the electron-donating triphenylamine unit, was observed in cyclic voltammogram of PTPAMSi. The HOMO energy level was estimated as -5.29 eV from the onset of the oxidation with regard to the energy level of the ferrocenium/ferrocene couple (Fc^+/Fc) (4.8 eV below vacuum). The LUMO energy level was obtained by adding the optical E_g to the HOMO level (as shown in Table 1). The low HOMO energy level suggests that incorporation of the siloxane to triphenylamine hardly alters its electronic transition energies and energy levels, thus maintaining the excellent hole injection performance of triphenylamine and yet significantly enhancing the thermal and morphological stability.

Table 1. Physical properties of PTPAMSi

E_T (eV) [a]	HOMO (eV) [b]	LUMO (eV) [c]	T_g (°C) [d]	T_d (°C) [e]
2.9	-5.29	-1.74	63	377

[a]Triplet energy level; [b] Highest occupied molecular orbital; [c] Lowest unoccupied molecular orbital; [d] Glass-transition temperature determined by DSC; [e] Decomposition temperature determined by TGA at 5% weight loss.

Electroluminescent Properties

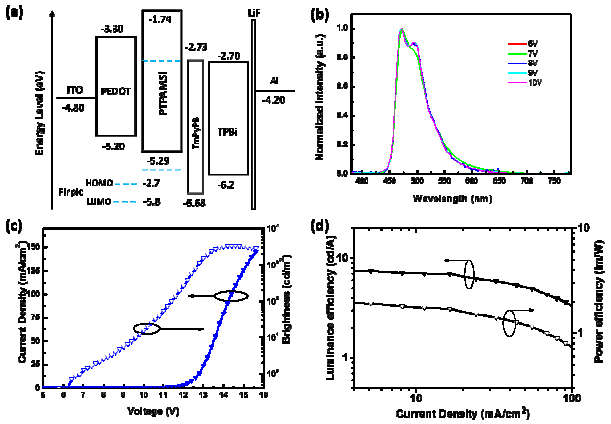

Fig. 4 (a) Device structure [ITO/ PEDOT:PSS (40 nm)/ PTPAMSi: 10 wt% FIrpic (40-45 nm)/ Tm3PyPB (5 nm)/ TPBi (30 nm)/ LiF (1 nm)/Al (100nm)] and the corresponding energy level diagram; (b) Normalized EL spectra of FIrpic based device adopting PTPAMSi as host with respect to voltage from 6 to 10 V. (c) *J-V-L* characteristics of a 10 wt% FIrpic-doped PhOLED; (d) Luminance efficiency and power efficiency versus current density of FIrpic-doped PhOLED.

To evaluate the utility of PTPAMSi as a host material for blue phosphor FIrpic, a blue spin-coating device was fabricated using FIrpic as phosphorescent emitter with the configuration of ITO/ PEDOT:PSS (40 nm) / PTPAMSi: 10 wt% FIrpic (30 nm) / Tm3PyPB (5 nm) / TPBi (30 nm) / LiF (1 nm) / Al (100 nm). PEDOT:PSS and LiF served as hole- and electron-injecting layers, respectively; The emitting layer was spin-coated from chlorobenzene solution on the PEDOT:PSS smoothed ITO glass substrate. Tm3PyPB[27] and TPBi were used as the hole/exciton-blocking and electron-transporting, respectively. Figure 4a depicts the relative energy levels of the materials employed in the devices. The EL spectrum of the device employing PTPAMSi as host with respect to voltage from 6 to 10 V is shown in Figure 4b. The Commission International de I'Eclairage (CIE) coordinates is exhibited in Table 2. Within all of the applying voltages it shows the same main peak at 475 nm with a shoulder peak at 500 nm, arising from the typical emitting of the phosphor FIrpic. This indicated that reverse transfer of triplet excitons from phosphor to host was prevented, and no emissions were observed other than the FIrpic emission.

Table 2. Performance of FIrpic-based device

V_{on} (V) [a]	L_{max} (cd/m2) [b]	$\eta_{c,max}$ (cd/A) [c]	$\eta_{p,max}$ (lm/W) [d]	$\eta_{ext,max}$ (%)[e]	CIE(x,y) [f]
6.8	3326	7.6	1.9	3.8	0.16,0.34

[a] Turn-on voltage; [b] Maximum luminance; [c] Maximum luminous efficiency; [d] Maximum power efficiency; [e] External quantum efficiency; [f] Commission Internationaledel'Eclairage coordinates.

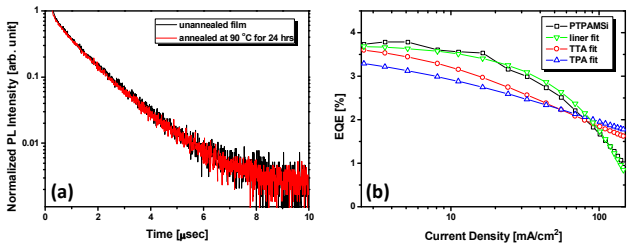

Fig. 5 (a) Transient photoluminescence decay (excited at 343 nm) curves at room temperature at 475 nm for the unannealed 10 wt% FIrpic co-deposited with PTPAMSi and annealed film at 90 °C for 24h; (b) External quantum efficiency versus current density for this device and the curve is fitted according to linear model and TTA, TPA model.

To further verify the exciton confinement property of the host, transient photoluminescence decays at a wavelength of 475 nm of thin film (formed on quartz substrates) with 10 wt% FIrpic dispersed in PTPAMSi were measured. According to Figure 5, the emission of films both display nearly mono-exponential decay curves, indicating that the triplet energy transfer from FIrpic to hosts is completely suppressed and the energy is well confined in emission layer. Meanwhile, the decay curve of the corresponding film annealed at 90 °C for 24 hours was nearly unchanged which suggests the thermal stability of the FIrpic doped film.

Table 3. Parameters determined from theory models and experiment

Slope[a]	k_{tt}[b]	k_p[c]	J_0 m [d]	J_0p [e]
0.019	$2.3*10^{-11}$	$7.9*10^{-15}$	83.4	90.3

[a]Slope of efficiency roll-off; [b]The rate governing the TTA reaction (cm^3 s^{-1}); [c]The rate governing TPA reaction (cm^3 s^{-1}); [d]The onset current density at EQE=EQE_0/2 (mA cm^{-2}); [e]The predicted value from TTA model (mA cm^{-2}).

To gain insight into the factor that affects the efficiency roll off, we characterized external quantum efficiency vs. current density by lin-log scale and used linear fit to determine the slope of roll off (Table 3). For phosphorescent OLEDs, the efficiency roll-off is mostly influenced by triplet-triplet annihilation (TTA) and triplet-polaron annihilation (TPA) process.[28] Previously, Steponas Raisys et al. have investigated roll-off in blue phosphorescent OLEDs based on polymeric hosts and TTA model is found to be mostly relevant to the efficiency roll-off.[29] In our PTPAMSi based device, we also fitted that with TTA and TPA model as shown in Figure 5b. It was observed that the fit of TTA model was much better than TPA one and the J_0 value predicted from TTA model was comparable to that determined by experiment. However, at low current density the experimental value was higher than the model curve, and at higher current density experimental value declined quicker than model predicted. We could deduce that from charge imbalances at low voltage, since the energy barriers inside the layer stack are different for electrons and holes. At higher current density and applied voltage, this imbalance decreases. But in our polymer device, field-induced quenching may occur because high applied voltage is need to run the device, which can be confirmed by the reduction of brightness vs. voltage (14 V).

Experimental Section

Materials

The intermediate methyldiethyoxylchlorosilane was prepared according to our previous report. All reactants (Adamas-beta) were purchased from Adamas Reagent, Ltd. without further purification and all solvents were supplied by Beijing Chemical Reagent Co., Ltd. Anhydrous and deoxygenated solvents were obtained by distillation over sodium benzophenone complex.

Device Fabrication

PhOLEDs: The hole-injection material PEDOT:PSS, electron-transporting and hole-blocking material TPBi, were used from commercial sources. ITO-coated glass with a sheet resistance of 10 Ω $square^{-1}$ was used as the substrate. Before device fabrication, the ITO-coated glass substrate was precleaned carefully and exposed to UV-ozone for 2 min. After that, PEDOT:PSS was spin-coated to the clean ITO substrate as hole-injection layer. Then, the host PTPAMSi doped with 10 % (by weight) FIrpic was spin-coated to form a 40 nm thick emissive layer (EML) and annealed at 100 °C for 30 min to remove residual solvent. Finally a 5 nm-thick hole-blocking layer (HBL) of Tm3PyPB and 30 nm-thick electron-transporting layer (ETL) of TPBi were vacuum deposited, and a cathode composed of a 1 nm-thick layer of lithium fluoride (LiF) and aluminum (100 nm) was sequentially deposited onto the substrate through shadow masking with a pressure of 10^{-6} Torr. The current density-voltage-luminance (*J-V-L*) characteristic of the device was measured using a Keithley 2400 Source meter and a Keithley 2000 Source multimeter equipped with a calibrated Si-photodiode in a glove box. The EL spectra were measured using a JY SPEX CCD 3000 spectrometer. The EQE values were calculated from the luminance, current density, and electroluminescence spectrum according to previously reported methods.[30] All measurements were performed at room temperature under ambient condition.

Characterization: ^{1}H NMR and ^{13}C NMR spectra were recorded on a Bruker AV400 (400MHz) spectrometer. Chemical shifts (δ) are given in parts per million (ppm) relative to tetramethylsilane (TMS; δ=0) as the internal reference. ^{1}H NMR spectra data are reported as chemical shift, relative integral, multiplicity (s = singlet, d = doublet, m = multiplet), coupling constant (*J* in Hz) and assignment. Elemental analyses of carbon, hydrogen, and nitrogen were performed on a Vario EL cube. UV-Vis absorption spectra were recorded on a Shimadzu UV-3600 recording spectrophotometer. PL spectra were recorded on a Hitachi F-7000 fluorescence spectrophotometer. Differential scanning calorimetry (DSC) was performed on a TA Q2000 Differential Scanning Calorimeter at a heating rate of 10 ^oC min^{-1} from 25 to 200 ^oC under nitrogen atmosphere. The glass transition temperature (Tg) was determined from the second heating scan. Thermogravimetric analysis (TGA) was undertaken with a METTLER TOLEDO TGA/DSC 1/1100SF instrument. The thermal stability of the samples under a nitrogen atmosphere was

determined by measuring their weight loss while heating at a rate of 10 °C min^{-1} from 25 to 800 °C. Cyclic voltammetry (CV) was carried out in nitrogen-purged CH_3CN (oxidation scan) at room temperature with a CHI voltammetric analyzer. Tetrabutylammoniumhexafluorophosphate (TBAPF6) (0.1 M) was used as the supporting electrolyte. The conventional three-electrode configuration consists of a glassy carbon working electrode, a platinum wire auxiliary electrode, and an $Ag/AgNO_3$ pseudo-reference electrode with ferrocenium-ferrocene (Fc^+/Fc) as the internal standard. Cyclic voltammograms were obtained at scan rate of 100 mV s^{-1}. The onset potential was determined from the intersection of two tangents drawn at the rising and background current of the cyclic voltammogram.

Theory Models:

To explain the efficiency roll-off of PTPAMSi based blue phosphorescent device, we use the following models:

Triplet-triplet annihilation (TTA):

The annihilation of two triplet states is possible via the following process: [31]

$$T_1 + T_1 \xrightarrow{k_{TT}} T_1 + S_0$$

here T_1 is an excited triplet on a dopant molecule, S_0 is a dopant molecule in the ground state, and k_{TT} is the rate governing the TTA reaction.

Under steady-state conditions, the quantum efficiency of the device (EQE) can be derived:

$$\frac{EQE}{EQE_0} = \frac{J_0}{4J}\left(\sqrt{1+\frac{8J}{J_0}} - 1\right) \quad (1)$$

with

$$J_0 = \frac{4ed}{k_{TT}\tau^2}$$

where e is the electron charge and d is the thickness of the exciton formation zone. EQE_0 is the quantum efficiency in the absence of TTA taken to be the maximum value of the efficiency curve. J_0 is the onset current density at $EQE=EQE_0/2$. It can be determined experimentally and also calculated by fitting equation (1) to EQE vs. current density curve. J_0 evaluation will provide the test of validity of our fitting. τ is triplet lifetime which is evaluated using photoluminescence (PL) transient measurement.

Triplet-polaron annihilation (TPA):

The annihilation of excited triplet states with free or trapped charge carriers is possible via the following process:[32]

$$T_1 + e^- / h^+ \xrightarrow{k_p} S_0 + e^{-*} / h^{+*}$$

here e^-/h^+ denotes electrons or holes and the star denotes higher excited states.

TPA is described by the following equation:

$$\frac{EQE}{EQE_0} = \frac{1}{1 + k_p / k_m C J^{1/(1+l)}} \quad (2)$$

where k_p is the TPA rate and parameter C describes the macroscopic properties of the system that can only be estimated (mobility and dielectric constant). The exciton recombination zone was considered to be 50 nm-thickness of the doped zone. C was considered to be 10^{19} cm $A^{-1/2}$, taking typical values of ε=3.5, μ=1*10^{-6} cm^2 V^{-1} s^{-1} and $l=E_t/k_T=1$(E_t depth of trap states) for organic semiconductors in line with Reineke et al. evaluations.[33]

Synthetic procedures

4-(diethoxy(methyl)silyl)-N,N-diphenylaniline (2): Under the argon atmosphere, chlorodiethoxy(methyl)silane (4.8 mL, 20 mmol) and magnesium powder (0.48 g, 20 mmol) were added in 30 mL anhydrous THF. The reaction flask was heated to 70 °C and a solution of 4-bromo-N,N-diphenylaniline (6.48 g, 20 mmol) in 50 mL of THF was added dropwise slowly within 30 minutes. After the addition completed, the mixture was stirred for 3h when keeping this temperature. Then it was cooled to room temperature and extracted with Et_2O. The solvent was evaporated in vacuo to give the crude product, which was purified by column chromatography on silica gel using (petroleum ether: dichloromethane = 4:1) as the eluent to obtain the product as colorless oil (3.99 g, 53 %). ^{1}H NMR (400 MHz, $CDCl_3$, δ): 0.37 (s, 3H, $-CH_3$), 1.27 (t, *J* = 7Hz, 6H; $-OCH_2CH_3$), 3.86 (q, *J* = 7Hz, 4H; $-OCH_2$), 7.06 (d, *J* = 8Hz, 4H; Ar H), 7.13 (d, *J* = 7Hz, 4H; Ar H), 7.28 (t, *J* = 8Hz, 4H; Ar H), 7.48 (d, *J* = 2Hz, 4H; Ar H). ^{13}C NMR (400 MHz, $CDCl_3$, δ): -1.97 20.48 60.55 124.15 125.32 126.97 129.42 131.36 137.11 149.55 151.50. ^{29}Si-NMR (400 MHz, $CDCl_3$, δ): -17.36. Anal. Calcd for C23H27NO2Si: C, 73.17; H, 7.21; N, 3.71. Found: C, 73.19; H, 7.20; N, 3.69.

PTPAMSi (4): To a mixture of 4-(diethoxy(methyl)silyl)-N,N-diphenylaniline (1.0 g, 2.65 mmol) and THF 100 mL, water (2 mL) and two drops of 1M HCl was added. The mixture was stirred at 0 °C for 24 h. After the reaction completed, the solvent was extracted with Et_2O and washed with distilled water for 3 times and dried over anhydrous magnesium sulfate. The filtrate was condensed by reduced pressure to give OH-Si monomer. Followed by adding a solution of 4-(diethoxy(methyl)silyl)-N,N-diphenylaniline (1.0 g, 2.65 mmol) in 50 mL THF and two drops of tetra-n-butyl titanate as catalyst. The mixture was stirred at 80 °C for a week by tracking the degree of reaction with Fourier Transform Infrared (FTIR) Spectrometer. After the reaction completed, 0.2 mL trimethylchlorosilane was added and stirred for another 12 h, white powder was finally obtained. ^{1}H NMR (400 MHz, $CDCl_3$, δ): 0.27 (brs, 3H; $-CH_3$), 7.0(brs, 8H; ArH), 7.18 (brs, 4H; ArH), 7.38 (brs, 2H; ArH).GPC (RI, polystyrene calibration) M_w = 9.34 x 10^3, M_w/M_n = 1.51.

Conclusions

In summary, a triphenylamine based polysiloxane was designed and synthesized successfully through incorporating triphenylamines side groups into a polysiloxane backbone. It exhibits excellent thermal and morphological stability for blue phosphorescent emitter FIrpic. Because silicon-oxygen bonds disrupt the π conjugation, PTPAMSi possesses a high E_T of 2.9 eV. The PTPAMSi maintains the physical appearance of polysiloxanes while adopting the photophysical and electrochemical characteristics of the triphenylamine. A device containing PTPAMSi as a host exhibits good performance.

Acknowledgements

The financial supports of NSFC (No. 21104002, 51221002 & 21006001), Beijing Higher Education Young Elite Teacher Project (YETP0491) and the Research Fund for the Doctoral Program of Higher Education (No. 20100010120001) are gratefully acknowledged. Z. R. thanks the China Scholarship Council for funding a visit to Durham University.

Notes and references

[a]*State Key Laboratory of Chemical Resource Engineering, Beijing University of Chemical Technology, Beijing 100029, China. E-Mail: skyan@mail.buct.edu.cn or renzj@mail.buct.edu.cn*

[b]*Beijing Key Laboratory of Membrane Science and Technology, Beijing University of Chemical Technology, 100029, China. E-Mail: liujt@mail.buct.edu.cn*

[c]*State Key Laboratory of Polymer Physics and Chemistry, Changchun*

Institute of Applied Chemistry, Chinese Academy of Sciences, Changchun, 130022, China

1. C. Fan, F. Zhao, P. Gan, S. Yang, T. Liu, C. Zhong, D. Ma, J. Qin, C. Yang, *Chem. Eur. J.* 2012, **18**, 5510
2. M. Talarico, R. Termine, E. M. Garcíá-Frutos, A. Omenat, J. L. Serrano, B. Gomez-Lor, A. Golemme, *Chem. Mater.* 2008, **20**, 6589
3. T. P. Bender, J. F. Graham, J. M. Duff, *Chem. Mater.* 2001, **13**, 4105.
4. K. Meerholz, *Nature* 2005, **437**, 327
5. A. A. Zakhidov, J. K. Lee, H. H. Fang, J. A. DeFranco, M. Chatzichristidi, P. G. Taylor, C. K. Ober, G. G. Malliaras, *Adv. Mater.* 2008, **20**, 3481.
6. M. J. Gretton, B. A. Kamino, T. P. Bender, *Macromol. Symp.* 2013, **324**, 82-94
7. B. A. Kamino, B. Mills, C. Reali, M. J. Gretton, M. A. Brook, and T. P. Bender, *J. Org. Chem.* 2012, **77**, 1663-1674
8. B. A. Kamino, J. B. Grande, M. A. Brook, T. P. Bender, *Org. Lett.* 2011, **13**, 154-157
9. L. Li, Z. Yu, W. Hu, C. H. Chang, Q. Chen, Q. Pei, *Adv. Mater.* 2011, **23**, 5563-5567.
10. H. Zhen, K. Li, Z. Huang, Z. Tang, R. Wu, G. Li, X. Liu, F. Zhang, *Appl. Phys. Lett.* 2012, **100**, 213901
11. D. J. Lipomi, B. C. K. Tee, M. Vosgueritchian, Z. Bao, *Adv. Mater.* 2011, **23**, 1771
12. Q. Huang, J. Li, T. J. Marks, G. A. Evmenenko, P. Dutta, *J. Appl. Phys.* 2007, **101**, 093101
13. D. Wright, U. Gubler, W. E. Moerner, M. S. DeClue, J. S. Siegel, *J. Phys. Chem. B* 2003, **107**, 4732-4737.
14. D. Kessler, M. C. Lechmann, S. Noh, R. Berger, C. Lee, J. S. Gutmann, P. Theato, *Macromol. Rapid Commun.* 2009, **30**, 1238-1242
15. S. Lamansky, P. Djurovich, D. Murphy, F. Abdel-Razzaq, H. E. Lee, C. Adachi, P. E. Burrows, S. R. Forrest, M. E. Thompson, *J. Am. Chem. Soc.* 2001, **123**, 4304-4312.
16. Y. Kawamura, K. Goushi, J. Brooks, J. J. Brown, H. Sasabe, C. Adachi, *Appl. Phys. Lett.* 2005, **86**, 071104.
17. A. Chaskar, H. F. Chen, K. T. Wong, *Adv. Mater.* 2011, **23**, 3876-3895.
18. M. Baldo, S. Lamansky, P. Burrows, M. Thompson, S. R. Forrest, *Appl. Phys. Lett.* 1999, **75**, 4-6.
19. C. Adachi, M. A. Baldo, M. E. Thompson, S. R. Forrest, *J. Appl. Phys.* 2001, **90**, 5048
20. M. Sudhakar, P. I. Djurovich, T. E. Hogen-Esch, M. E. Thompson, *J. Am. Chem. Soc.* 2003, **125**, 7796-7797.
21. Z. Ge, T. Hayakawa, S. Ando, M. Ueda, T. Akiike, H. Miyamoto, T. Kajita, M. Kakimoto, *Adv. Funct. Mater.* 2008, **18**, 584-590.
22. M. J. Gretton, B. A. Kamino, M. A. Brook, T. P. Bender, *Macromolecules* 2012, **45**, 723-728
23. Y. Lim, Y. Park, Y. Kang, D. Y. Jang, J. H. Kim, J. J. Kim, A. Sellinger, D. Y. Yoon, *J. Am. Chem. Soc.* 2011, **133**, 1375-1382
24. X. Liu, C. Zheng, M. F. Lo, J. Xiao, C. Lee, M. K. Fung, X. Zhang, *Chem. Commun.* 2014, **50**, 2027-2029
25. C. Halkyard, M. Rampey, L. Kloppenburg, S. Studer-Martinez, U. Bunz, *Macromolecules* 1998, **31**, 8655-8659.
26. J. E. Mark, *Acc. Chem. Res.* 2004, **37**, 946-953.
27. S.-J. Su, Y. Takahashi, T. Chiba, T. Takeda, J. Kido, *Adv. Mater.* 2009, **19**, 1260-1267.
28. C. Murawski, K. Leo, M. C. Gather, *Adv. Mater.* 2013, **25**, 6801-6827
29. E. Stanislovaityte, J. Simokaitiene, S. Raisys, H. Al-Attar, J. V. Grazulevicius, A. P. Monkman, V. Jankus, *J. Mater. Chem. C* 2013, **1**, 8209-8221
30. S. Forrest, D. Bradley and M. Thompson, *Adv. Mater.* 2003, **15**, 1043-1048.
31. M. A. Baldo, C. Adachi and S. R. Forrest, *Phys. Rev. B: Condens. Matter Mater. Phys.* 2000, **62**, 10967
32. J. Kalinowski, W. Stampor, J. Mezyk, M. Cocchi, D. Virgili, V. Fatori, P. D. Marco, *Phys. Rev. B* 2002, **66**, 235321
33. S. Reineke, K. Walzer, K. Leo, *Phys. Rev. B: Condens. Matter Mater. Phys.* 2007, **75**, 125328

Triphenylamine based polysiloxane has been successfully synthesized as phosphorescent host. This work demonstrates that modifying triphenylamine by polysiloxane is a promising approach to improve the its physical properties while maintain its electronic properties.